Minimizing the number of mobile chargers for large-scale wireless rechargeable sensor networks ☆

Haipeng Dai *, Xiaobing Wu, Guihai Chen, Lijie Xu, Shan Lin

State Key Laboratory for Novel Software Technology, Nanjing University, Nanjing 210023, PR China

ARTICLE INFO

ABSTRACT

Traditional wireless sensor networks (WSNs) are constrained by limited battery energy that powers the sensor nodes, which impedes the large-scale deployment of WSNs. Wireless power transfer technology provides a promising way to solve this problem. With such novel technology, recent works propose to use a single mobile charger (MC) traveling through the network fields to replenish energy to every sensor node so that none of the nodes will run out of energy. These algorithms work well in small-scale networks. In large-scale networks, these algorithms, however, do not work efficiently, especially when the amount of energy the MC can provide is limited. To address this issue, multiple MCs can be used. In this paper, we investigate the minimum MCs problem (MinMCP) for two-dimensional (2D) wireless rechargeable sensor networks (WRSNs), i.e., how to find the minimum number of energy-constrained MCs and design their recharging routes in a 2D WRSN such that each sensor node in the network maintains continuous work, assuming that the energy consumption rate for all sensor nodes are identical. By reduction from the Distance Constrained Vehicle Routing Problem (DVRP), we prove that MinMCP is NP-hard. Then we propose approximation algorithms for this problem. Finally, we conduct extensive simulations to validate the effectiveness of our algorithms.

© 2014 Elsevier B.V. All rights reserved.

1. Introduction

Wireless sensor networks (WSNs) have been widely used for structural health monitoring, scientific exploration, environmental monitoring, target tracking, etc. As sensor nodes in traditional WSNs are powered by batteries, the limited battery energy is considered as a major deployment barrier for large-scale WSNs. To elongate the lifetime of WSNs, many approaches have been proposed to harvest ambient energy from their surroundings such as solar energy [2], vibration energy [3], and wind energy [4]. However, due to the time-varying nature of renewable energy resources, the success of these methods remains very limited in practice.

The recent breakthroughs in wireless power transfer technology [5], which allow energy to be transferred from one storage device to another via wireless with reasonable efficiency, has provided a promising way to solve this problem. Since wireless recharging can guarantee the continuous power supply and is insensitive to the neighboring environment, it has found many applications

including RFIDs [6], sensors [7], cell phones [8], laptops [9], vehicles [10], smart grids [11] and civil structures monitoring [12]. With the novel technology, recent studies [12–18,1] propose to employ a mobile charger (MC) to replenish energy to sensor nodes in wireless rechargeable sensor networks (WRSNs) [19–21] so that none of them in the network will run out of energy. Typically, the MC periodically traverses every node in the network and stays near every node for a short period to recharge it. Research results demonstrate that this approach works well for small-scale networks. For large-scale wireless sensor networks, a single mobile charger may not be enough. This is because the MC may not carry sufficient energy to recharge every node in a large-scale network on a single tour. Therefore, the MC needs to return to the base station after recharging a part of the network. As a result, single MC recharging algorithms become invalid and continuous working of sensor nodes can no longer be guaranteed.

To recharge a large-scale sensor network, it is necessary to use multiple energy constrained mobile chargers. In this work, we investigate the minimum mobile charger problem for wireless sensor networks. That is, how to find the minimum number of energy-constrained MCs as well as their routes to recharge a given WRSN such that each sensor node in the WRSN can work continuously. In our problem settings, the energy consumption rate for all sensor nodes are identical, which is a practical assumption for many

---

applications as will be elaborated. This problem is highly challenging as we should jointly consider the energy constraints of MCs and the time-sensitive charging requirements of sensor nodes when determining the routes of MCs. We prove the NP-hardness of this problem and propose efficient approximation algorithms to solve it. Zhang et al. [22] also employed multiple energy-constrained MCs. However, their work focuses on only one-dimensional (1D) sensor networks, and their goal is to maximize the ratio of the amount of payload energy to the overhead energy. Our solution is designed for two-dimensional (2D) sensor networks, and concentrates on an entirely different problem compared with [22].

The contributions of this work are as follows.

- We are the first to consider the minimum mobile chargers problem (MinMCP) in general 2D WRSNs, i.e., how to find the minimum number of energy-constrained MCs and their recharging routes given a 2D WRSN, so as to keep the network running forever.
- We prove that MinMCP is NP-hard, and propose approximation algorithms to address MinMCP. Particularly, we first consider the relaxed version of MinMCP, which is named MinMCP-R, and propose an approximation algorithm to address it. Furthermore, we present approximation algorithms to MinMCP based on the results obtained for MinMCP-R.
- We conduct extensive simulations to verify our analytical findings. The simulation results demonstrate the effectiveness of our schemes.

The remainder of the paper is organized as follows. In Section 2, we investigate some related works. We present preliminaries and background in Section 3. In Section 4, we first formulate the problem and investigate its hardness. Then we propose approximation algorithms and conduct performance analysis respectively. Section 5 discusses how to extend our work to general cases. Experimental results are presented in Section 6 before we conclude the paper in Section 7.

2. Related work

In this section, we review some related works in terms of mobile charging problems where a single or multiple MCs are used.

There has emerged a considerable amount of work studying how to use one single MC to enhance the performances of WRSNs. In terms of data routing performance, Tong et al. [13] investigated the impact of wireless charging technology on data routing and deployment of sensor networks where a single MC is applied. A more practical scheme jointly considering routing and charging was reported in [15]. It aimed to maximize the network lifetime under practical constraints such as dynamic and unreliable communication environment, limited charging capability and heterogeneous node attributes. Other works were interested in the impact of mobile charging on the efficiency of data gathering. Shi et al. [14] employed an MC to periodically travel inside the sensor network to charge sensor nodes, and tried to minimize the aggregate charging time and travel time. By [23,24], a mobile charger was used to serve not only as an energy transporter that charges stationary sensors, but also as a data collector. In addition, Xie et al. [25] studied the problem of co-locating the mobile base station on the wireless charging vehicle to minimize energy consumption of the entire system while guaranteeing that none of the sensor nodes will run out of energy. Still others concentrated on stochastic event capture issues. Dai et al. [18] considered two closely related subproblems of mobile charging for stochastic event capture. One is how to choose the nodes for charging and decide the charging time for each of them, and the other is how to best

schedule the nodes' activation schedules according to their received energy. Their goal is to maximize the overall quality of monitoring.

Besides the above concerns on traditional performances of sensor networks, some literature paid attention to practical issues related to the MC. Fu et al. [26] focused on minimizing the charging delay of the MC, an RFID-reader, by planning its optimal movement and charging strategy. While most existing works on the mobile charging problem mainly concentrated on the optimal offline path planning for the MC, He et al. [27] considered the on-demand mobile charging problem, i.e., how to dynamically plan the path for the MC where the charging requests from sensor nodes come randomly. Li et al. [16] tried to maximize the number of sensor nodes to be charged by using a single MC with limited energy, which is different from the above schemes that assume the employed MC has unbounded energy.

In order to charge a large-scale WRSN, multiple MCs are needed considering their energy constraint. Zhang et al. [22] proposed the only scheme employed multiple energy-constrained MCs to collaboratively charge a linear WSN. MCs are allowed to charge each other. Their goal is to maximize the energy efficiency of charging, which is totally different from ours.

3. Problem statement

3.1. Network model

We assume that there is a collection of rechargeable sensor nodes distributed over a 2D region. A base station (BS) serves not only as a data sink, but also as an energy source of the network by periodically dispatching MCs to charge the sensor nodes, as illustrated in Fig. 1. Let $G = (V, E)$ represent the topology of sensor nodes and the BS. Let $v_{BS} \in V$ denote the BS, and $J = V \setminus v_{BS}$ ($|J| = n$) be the set of sensor nodes. Denote by $w(i,j)$ the time cost for MCs traveling from a sensor node v_i to another sensor node v_j, which we call the edge weight. Notice that $w(i,j)$ includes neither the charging time of MCs at the sensor node v_i nor that at the sensor node v_j. We assume that G is complete, and the edge weights form a metric space $\mathcal{W}$, namely, they are symmetric and satisfy the triangle inequality. To be specific, we have $w(i,j) = w(j,i)$ and $w(i,j) \leqslant w(i,k) + w(k,j)$ for arbitrary sensor nodes v_i, v_j and v_k. We emphasize that this assumption is without loss of generality because an MC can always travel along the shortest path between any two sensor nodes (e.g., if $w(i,j) > w(i,k) + w(k,j)$, an MC will prefer to travel from i to j by passing by k, which results in an
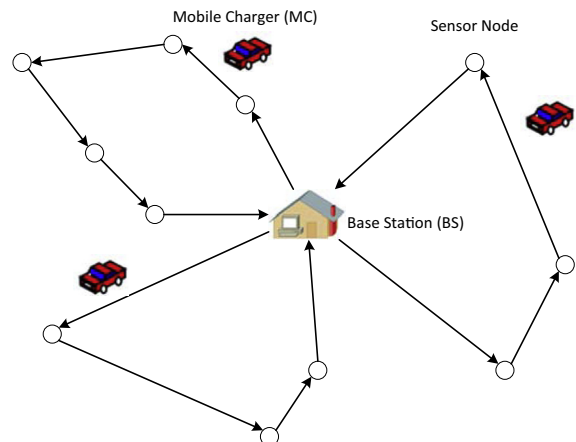

Fig. 1. Illustration of the network model.

equivalent edge weight between i and j, $w'(i,j) = w(i,k) + w(k,j)$, which leads to inherent triangle inequality among nodes.

Every sensor node has a battery capacity of E_{max}, and needs a minimum energy E_{min} to be operational. We assume that the energy consumption rate is constant and uniform for all sensor nodes, and is denoted by p_w. This assumption holds for a number of scenarios. For example, Jiang et al. [28] studied wireless power transmission for sensor nodes buried inside concrete. These sensor nodes collect valuable volumetric data related to the health of a structure, and wirelessly transmit the data to a data collection receiver directly [29]. As their transmitting power is uniform, the energy consumptions of the sensor nodes are identical to each other. In [12][30], a civil structure is instrumented with sensor nodes capable of being charged wirelessly by a mobile helicopter, which also serves as a data collector. Thus, hop-by-hop data transmissions are no longer needed, and the energy consumptions can be conserved and balanced on sensor nodes. In addition, RFID sensors in Wireless Identification and Sensing Platform (WISP) [26,31,32] typically consume energy at the same rate, and they can be wirelessly charged by a mobile charger [33].

A summary of the notations in this paper is given in Table 1.

3.2. Charging model

Suppose that a fully charged MC k starts from the BS and visits every node of a subset of sensor nodes $S_k \subseteq J$ exactly once and charges them. The MC k spends τ_i^k units of time in charging a node v_i. Denote the tour of the MC k by $P_k = (\pi_0, \pi_1, \ldots, \pi_{|S_k|}, \pi_{|S_k|+1})$ where $\pi_0 = \pi_{|S_k|+1} = v_{BS}$ and $\{\pi_i\}_{i=1}^{|S_k|} = S_k$. Consequently, the time the MC k takes to travel along P_k is given by $\tau_P^k = \Sigma_{i=0}^{|S_k|} w(\pi_i, \pi_{i+1})$.

Table 1
Notations used.

Symbol	Meaning
$w(i,j)$	Time cost for MCs traveling from node v_i to v_j
E_{max}	Battery capacity for all sensor nodes
E_{min}	Minimum energy for sensor nodes to be operational
p_w	Energy consumption rate for all sensor nodes
$\mathcal{M}$	Set of tours of all MCs
τ_i^k	Charging time allocated to node v_i by the MC k
τ_P^k	Travel time of the MC k
τ_{vac}^k	Vacation time of the MC k
τ_{vac}^c	Minimum required vacation time for MCs
τ^k	Time period of recharge schedule for the MC k
U	Energy transfer rate of MCs
B	Battery capacity of MCs
η_C	Working Power of MCs for Traveling
η_T	Working Power of MCs for Charging

Further, let $\mathcal{M}$ be the set of tours of all MCs, which means that $P_k \in \mathcal{M}$ and $k \in [|\mathcal{M}|]$ for any MC k.

After finishing the charging, The MC k returns to the BS to be serviced (e.g., replacing or recharging its battery) and gets ready for the next trip. This period is called *vacation time*, and is denoted as τ_{vac}^k. We demand that τ_{vac}^k for any MC k should not be smaller than a given constant value τ_{vac}^c, i.e.,

$$\tau_{vac}^k \geqslant \tau_{vac}^c \quad (k \in [|\mathcal{M}|]), \tag{1}$$

in order to meet the requirements of most applications. The MC k repeats its recharge schedule every period of time τ^k, which consists of charging time, travel time and vacation time, i.e.,

$$\tau^k = \tau_P^k + \tau_{vac}^k + \Sigma_{v_i \in S_k} \tau_i^k \quad (k \in [|\mathcal{M}|]). \tag{2}$$

Let U $(U > p_w)$ be the energy transfer rate of an MC during charging. To ensure that each sensor node maintains continuous work and the charging cost of an MC is minimized, the renewable energy cycle of each sensor node should be guaranteed [14]. In particular, the energy level of a sensor node $v_i \in J$ exhibits a renewable energy cycle if it satisfies the following two requirements: (i) it starts and ends with the same energy level over a period of τ^k; and (ii) it never falls below E_{min}. Mathematically, the following two conditions should be satisfied.

$$\tau^k \cdot p_w = \tau_i^k \cdot U \quad (k \in [|\mathcal{M}|], v_i \in S_k), \tag{3}$$

$$E_{max} - (\tau^k - \tau_i^k) \cdot p_w \geqslant E_{min} \quad (k \in [|\mathcal{M}|], v_i \in S_k). \tag{4}$$

The first equation indicates that the amount of energy charged to a node v_i during τ_i must be equal to that consumed by v_i in a schedule period, and the second inequality is obtained by considering the lowest energy level of the node.

We take Fig. 2 as an example. The energy level of sensor node 1 during the first three renewable cycles (marked in the solid sawtooth graph) has only two slopes: one is $-p_w$ when no MC charges this node during this time period, and the other is $U - p_w$ when an MC is charging this node at a rate of U. Also shown in Fig. 2 is another renewable energy cycle (marked in the dashed sawtooth graph) of sensor node 2, where the battery energy is charged to E_{max} during an MC's visit and falls to the lowest energy level of E_{min} in non-charging period. Note that the time period of node 1 differs from that of node 2. This is because they are charged by different MCs with different recharge schedules. For more details of the renewable energy cycle, we refer the reader to [14].

Note that, on the contrary, the charging scheme in [22] requires all MCs to have uniform schedule periods, which means that the MCs finishing the charging tasks earlier have to wait at the BS for the returns of other MCs before starting the next trip. Consequently, to compensate the inefficiency of MCs caused by waiting, more MCs are needed compared with our scheme. Besides, we stress that our scheme can be easily extended to the case where
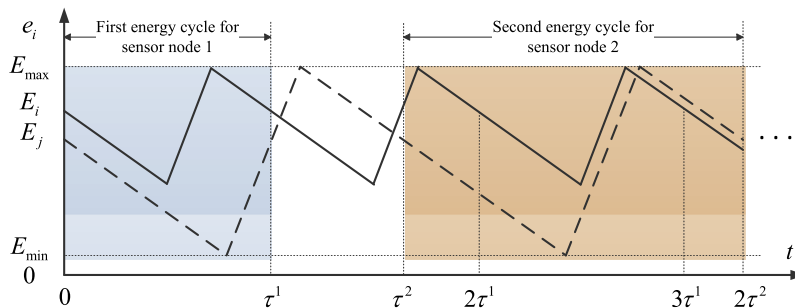

Fig. 2. Illustration of renewable energy cycles.

uniform schedule periods for MCs are mandatory. In fact, this case is much simpler to handle.

3.3. Energy consumption model for MCs

Suppose that each MC is energy-constrained and has an energy capacity of B. Furthermore, denote by η_C the working power of each MC during traveling, and η_T the working power of each MC when it stops and charges sensor nodes. For each MC, its movements and charging process share the same pool of battery energy. Clearly, the overall energy an MC spends in traveling and charging should not exceed its battery capacity B. That is,

$$\eta_T \cdot \tau_P^k + \eta_C \cdot \Sigma_{v_i \in S_k} \tau_i^k \leqslant B. \tag{5}$$

In most cases, η_T is much bigger than η_C, which means that the power spent in charging sensor nodes for an MC is typically far less than the power consumed in traveling. For example, the working power of the off-shelf product–TX91501 transmitter produced by Powercast is 3 W. When a vehicle (serves as an MC) equipped with such a power transmitter stops to charge a sensor node, the working power of the transmitter can be accounted as the unique energy consumption source, which is much less than the vehicle's traveling power.

But there are exceptions. For instance, the helicopter in [12] which serves as an MC might spend more energy when hovering for charging sensor nodes than that when flying, i.e., $\eta_C > \eta_T$. We include this case in the theoretical part.

3.4. Problem description

Definition 1 (*Minimum mobile chargers problem (MinMCP)*). Given a set of sensor nodes J with parameters p_w, E_{max} and E_{min}, the metric space $\mathcal{W}$ including the time cost of an MC to travel between any pair of nodes, find a minimum required number of MCs (with parameters η_C, η_T, U, B and τ_{vac}^c) originating at the BS and collectively visiting all the sensor nodes to charge them, such that none of the sensor nodes will run out of energy.

Combining Eqs. (1)(2)(3)(4), we can derive

$$\tau_P^k \leqslant (\alpha - \tau_{vac}^c) - \lambda \cdot \alpha \cdot |S_k| \quad (k \in [|\mathcal{M}|]) \tag{6}$$

and

$$\tau^k = \frac{\tau_P^k + \tau_{vac}^k}{1 - \lambda \cdot |S_k|} \quad (k \in [|\mathcal{M}|]), \tag{7}$$

where $\alpha = \frac{U \cdot (E_{max} - E_{min})}{p_w \cdot (U - p_w)}$ and $\lambda = \frac{p_w}{U}$.

Due to the fact that $\tau^k > 0$, we can immediately derive the following condition from Eq. (7)

$$|S_k| < \frac{1}{\lambda}. \tag{8}$$

Meanwhile, combining Eqs. (1)–(3) and (5), we have

$$\tau_P^k \leqslant \frac{B - \lambda \cdot (B + \eta_C \cdot \tau_{vac}^c) \cdot |S_k|}{\eta_T + \lambda \cdot (\eta_C - \eta_T) \cdot |S_k|} \quad (k \in [|\mathcal{M}|]). \tag{9}$$

To sum up, the problem in this paper can be formulated as follows.

Min $\quad |\mathcal{M}|$ $\tag{10}$
s.t. $\quad \tau_P^k \leqslant (\alpha - \tau_{vac}^c) - \lambda \cdot \alpha \cdot |S_k| \quad (k \in [|\mathcal{M}|])$

$$\tau_P^k \leqslant \frac{B - \lambda \cdot (B + \eta_C \cdot \tau_{vac}^c) \cdot |S_k|}{\eta_T + \lambda \cdot (\eta_C - \eta_T) \cdot |S_k|} \quad (k \in [|\mathcal{M}|]) \tag{11}$$

$$\cup_{k \in [|\mathcal{M}|]} S_k = J; \quad |S_k| < \frac{1}{\lambda}; \quad S_i \cap S_j = \emptyset \quad (i, j, k \in [|\mathcal{M}|], \ i \neq j)$$

where $\alpha = \frac{U \cdot (E_{max} - E_{min})}{p_w \cdot (U - p_w)}$ and $\lambda = \frac{p_w}{U}$.

Define $\quad f_1(|S_k|) = (\alpha - \tau_{vac}^c) - \lambda \cdot \alpha \cdot |S_k| \quad$ and $\quad f_2(|S_k|) = \frac{B - \lambda \cdot (B + \eta_C \cdot \tau_{vac}^c) \cdot |S_k|}{\eta_T + \lambda \cdot (\eta_C - \eta_T) \cdot |S_k|}$. For simplicity, we use $f_1(|S_k|)$ (or $f_2(|S_k|)$) to represent the constraint $\tau_P^k \leqslant f_1(|S_k|)$ (or $\tau_P^k \leqslant f_2(|S_k|)$), if there is no confusion. In addition, we assume that $2 \cdot w(v_{BS}, v_i) \leqslant f_1(1)$ and $2 \cdot w(v_{BS}, v_i) \leqslant f_2(1)$ for any node $v_i \in J$, otherwise there is no feasible solution for MinMCP.

4. Solving MinMCP: theoretical results and approximation algorithms

In this section, we first find that MinMCP is difficult to tackle directly after examining the hardness of MinMCP. Then, we resort to solve its relaxed version MinMCP-R. Finally, we come up with an approximation algorithm for MinMCP based on the solution to MinMCP-R.

4.1. Hardness of MinMCP

First, we review the following NP-complete problem.

Definition 2 (*Distance Constrained Vehicle Routing Problem (DVRP)* [34]). Given a set of vertices in a metric space, a specified depot, and a distance bound D, find a minimum cardinality set of tours originating at the depot that covers all vertices, such that each tour has length at most D.

The following theorem shows the hardness of MinMCP.

Theorem 4.1. *MinMCP is NP-hard.*

Proof. In general, we prove the NP-hardness of MinMCP by reducing from DVRP.

To begin with, let us consider a special case of MinMCP when $\eta_C = \eta_T$ and p_w is rather small such that $\lambda = \frac{p_w}{U} \approx 0$. Consequently, the two constraints of MinMCP (10) and (11) can be rewritten as $\tau_P^k \leqslant (\alpha - \tau_{vac}^c)$ and $\tau_P^k \leqslant \frac{B}{\eta_T}$, respectively. Meanwhile, the constraint of $|S_k|$, i.e., $|S_k| < \frac{1}{\lambda}$, can be safely removed. Further, let $\frac{B}{\eta_T} \leqslant (\alpha - \tau_{vac}^c)$ (this condition can be easily satisfied since $\alpha = \frac{U \cdot (E_{max} - E_{min})}{p_w \cdot (U - p_w)}$ is a very large number given that $\frac{p_w}{U} \approx 0$), the two constraints can thus be equivalently simplified as $\tau_P^k \leqslant \frac{B}{\eta_T}$. The resulting problem is clearly in the form of DVRP.

Formally, given any instance of DVRP with distance bound D, we can set $\frac{B}{\eta_T} = D, \eta_C = \eta_T$ as well as the values of the related parameters such that $\frac{p_w}{U} \approx 0$ and $\frac{B}{\eta_T} \leqslant (\alpha - \tau_{vac}^c)$, and thus obtain an instance of MinMCP. Such construction process, apparently, can be done in polynomial time. Since DVRP is NP-complete and thus is NP-hard, we then conclude that MinMCP is also NP-hard. □

4.2. Roadmap of our solution

Our roadmap to solve MinMCP is as follows. Due to the difficulty of tackling MinMCP directly, we first consider its relaxed version where the linear constraint $f_1(|S_k|)$ is removed, which we call MinMCP-R.

For MinMCP-R, we first relax the nonlinear constraint $f_2(|S_k|)$ into a linear one, and then reduce the problem to DVRP by applying a simple transformation. This approach enables us to propose an approximation algorithm.

Based on the solution to MinMCP-R, we can construct a feasible solution to MinMCP by taking into account the constraint $f_1(|S_k|)$ again. An approximation algorithm is also provided for this case.

4.3. Approximation algorithm for MinMCP-R

First of all, we define γ-Constant Transformation in metric space as follows.

Definition 3 (γ-Constant Transformation). Given a metric space $\mathcal{W}$ and a constant γ, the γ-Constant Transformation for $\mathcal{W}$ is to revise the weight $w(i,j)$ between any pair of sensor nodes v_i and v_j as $w(i,j) + \gamma$, and $w(i, v_{BS})$ between any sensor node v_i and the BS as $w(i, v_{BS}) + \gamma/2$.

We denote by Δ the maximum distance of any node from the BS, and $\Delta(\gamma)$ the corresponding one after the γ-Constant Transformation. It is easy to verify the following lemma.

Lemma 4.1. *The metric space after a γ-Constant Transformation is still metric.*

Proof. Denote by $\widetilde{w}(i,j)$ the edge weight between nodes v_i and v_j after the γ-Constant Transformation. On one hand, we have

$$\widetilde{w}(i,j) = w(i,j) + \gamma \leqslant (w(i,j) + w(j,k)) + 2 \cdot \gamma$$
$$\leqslant (w(i,k) + \gamma) + (w(k,j) + \gamma) \leqslant \widetilde{w}(i,k) + \widetilde{w}(k,j). \quad (12)$$

Note that the first inequality stems from the fact that the original space is metric and thus $w(i,j) \leqslant w(i,j) + w(j,k)$.

On the other hand, it is easy to see that

$$\widetilde{w}(i,j) = \widetilde{w}(j,i).$$

To sum up, the edge weights in the transformed space are symmetric and satisfy the triangle inequality. In other words, the transformed space is metric. This completes the proof. □

We propose our algorithm for MinMCP-R in Algorithm 1. Particularly, Algorithm 1 has different treatments for the case where $\eta_C \leqslant \eta_T$ and that where $\eta_C > \eta_T$.

Algorithm 1. Algorithm for MinMCP-R

Input: The metric space $\mathcal{W}$, the constraint $f_2(|S_k|)$, parameters
　　$\eta_C, \eta_T, \lambda, B$ and τ_{vac}^c
Output: The set of tours $\mathcal{M}$, the relaxed constraint $f_2^R(|S_k|)$
1 begin
2　**if** $\eta_C \leqslant \eta_T$ **then**
3　　　Apply $\frac{\lambda \cdot (B + \eta_C \cdot \tau_{vac}^c)}{\eta_T}$-Constant Transformation on $\mathcal{W}$;
4　　　Run the algorithm for DVRP [34] in the new metric space
　　　　with distance bound $\frac{B}{\eta_T}$, and get the set of tours $\mathcal{M}$;
5　　　Employ the Nearest Neighbor Algorithm for TSP on each
　　　　tour in $\mathcal{M}$ to further reduce its length;
6　　　$f_2^R(|S_k|) = \frac{B}{\eta_T} - \frac{\lambda \cdot (B + \eta_C \cdot \tau_{vac}^c)}{\eta_T} \cdot |S_k|$;
7　**else**
8　　　Apply $\frac{\lambda \cdot (B \frac{\eta_C}{\eta_T} + \eta_C \cdot \tau_{vac}^c)}{\eta_T}$-Constant Transformation on $\mathcal{W}$;
9　　　Run the algorithm for DVRP in the new metric space
　　　　with distance bound $\frac{B}{\eta_T}$, and get the set of tours $\mathcal{M}$;
10　　　Employ the Nearest Neighbor Algorithm for TSP on
　　　　each tour in $\mathcal{M}$ to further reduce its length;
11　　　$f_2^R(|S_k|) = \frac{B}{\eta_T} - \frac{\lambda \cdot (B \frac{\eta_C}{\eta_T} + \eta_C \cdot \tau_{vac}^c)}{\eta_T} \cdot |S_k|$;
12 end

In general, for each case, Algorithm 1 first applies a proper γ-Constant Transformation to construct a new metric space, and then employs the algorithm for DVRP on this metric space to obtain the set of tours. Briefly speaking, the algorithm for DVRP

proposed in [34] first divides the sensor nodes into several sets according to their distance to the BS. Next, it conducts the algorithm for unrooted DVRP [35] for each sensor node set and thus get a number of paths. Finally, it appends both end points of every path with edges from the BS to form tours.

After obtaining the tours, Algorithm 1 adopts the Nearest Neighbor Algorithm on each tour to refine the results, which repeatedly visits the nearest sensor node until all sensor nodes have been visited. This optimization step distinguishes the algorithm from Algorithm 1 proposed in [1].

One of the outputs of the algorithm is the relaxed constraint of $f_2(|S_k|)$, i.e., $f_2^R(|S_k|)$, a useful element in later sections. Note that at Step 5 and at Step 10, we employ the Nearest Neighbor Algorithm for TSP to further reduce the length of each obtained tour.

4.4. Analysis of the Approximation Algorithm for MinMCP-R

We give performance bounds of Algorithm 1 for three cases respectively, i.e., $\eta_C = \eta_T, \eta_C < \eta_T$ and $\eta_C > \eta_T$.

Theorem 4.2. *Given that $\eta_C = \eta_T$, Algorithm 1 for MinMCP-R achieves* $6 \cdot \left(\left\lceil \log_2 \frac{B/\eta_T}{B/\eta_T - 2\Delta\left(\frac{\lambda \cdot (B + \eta_C \cdot \tau_{vac}^c)}{\eta_T} \right) + 2} \right\rceil + 1 \right)$*-approximation.*

Proof. Given $\eta_C = \eta_T$, the constraint $f_2(|S_k|)$ can be simplified as:

$$\tau_P^k \leqslant \frac{B}{\eta_T} - \frac{\lambda \cdot (B + \eta_C \cdot \tau_{vac}^c)}{\eta_T} \cdot |S_k|. \quad (13)$$

Note that $\tau_P^k = \Sigma_{i=0}^{|S_k|} w(\pi_i, \pi_{i+1})$. Moreover, the weight of the same tour in the revised metric space after applying $\frac{\lambda \cdot (B + \eta_C \cdot \tau_{vac}^c)}{\eta_T}$-Constant Transformation on $\mathcal{W}$ in Algorithm 1 is given by:

$$\tau_P^{k'} = \left(w(v_{BS}, \pi_1) + \frac{1}{2} \cdot \gamma_1 \right) + \left(w(\pi_{|S_k|}, v_{BS}) + \frac{1}{2} \cdot \gamma_1 \right)$$
$$+ \Sigma_{i=1}^{|S_k|-1} (w(\pi_i, \pi_{i+1}) + \gamma_1) \quad (14)$$

where $\gamma_1 = \frac{\lambda \cdot (B + \eta_C \cdot \tau_{vac}^c)}{\eta_T}$. Combining Eqs. (13) and (14) and following the fact that $\tau_P^k = \Sigma_{i=0}^{|S_k|} w(\pi_i, \pi_{i+1})$, we have:

$$\tau_P^{k'} \leqslant \frac{B}{\eta_T}. \quad (15)$$

Thus, our problem is reduced to DVRP with distance bound $\frac{B}{\eta_T}$. According to Theorem 3 in [34], the result follows. □

Theorem 4.3. *Given that $\eta_C < \eta_T$, Algorithm 1 for MinMCP-R achieves* $6 \cdot \left(2 \cdot \frac{B + \eta_C \cdot \tau_{vac}^c}{B \frac{\eta_C}{\eta_T} + \eta_C \cdot \tau_{vac}^c} + 1 \right) \left(\left\lceil \log_2 \frac{B/\eta_T}{B/\eta_T - 2\Delta\left(\frac{\lambda \cdot (B + \eta_C \cdot \tau_{vac}^c)}{\eta_T} \right) + 2} \right\rceil + 1 \right)$*-approximation.*

Proof. First of all, it is easy to verify that $f_2(0) = \frac{B}{\eta_T}, f_2(|S_k|_2) = 0$ where $|S_k|_2 = \frac{B}{\lambda \cdot (B + \eta_C \cdot \tau_{vac}^c)}$, and $f_2(|S_k|)$ is a decreasing and concave function given that $\eta_C < \eta_T$ (we don't have to consider the case where $|S_k| \geqslant \frac{\eta_T}{\lambda \cdot (\eta_T - \eta_C)}$, since $|S_k| < \frac{1}{\lambda}$ is required for a feasible solution in MinMCP), as illustrated in Fig. 3. Also in Fig. 3, the line $f_2^R(|S_k|)$, one of the outputs of Algorithm 1, connects the two points of $f_2(|S_k|)$ at $|S_k| = 0$ and $|S_k| = |S_k|_2$. The other line, $g(|S_k|)$, is tangent to $f_2(|S_k|)$ at point $|S_k| = 0$, and intersects the horizontal axis at point $|S_k|_2^g = \frac{B}{\lambda \cdot (B \frac{\eta_C}{\eta_T} + \eta_C \cdot \tau_{vac}^c)}$.

A region in the first quadrant is said to be *feasible* if any point τ_P^k within it satisfies the constraint $f_2(|S_k|)$. In Fig. 3, both of the regions I and II are feasible, while the region III is not. Denote by
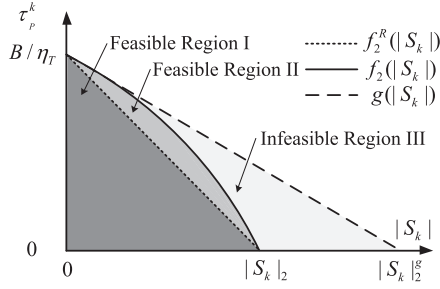
Fig. 3. Feasible region analysis for the case where $\eta_C < \eta_T$ in MinMCP-R.

$\mathcal{M}^{R*}$, $\mathcal{M}^*$ and $\mathcal{M}^{g*}$ the optimal sets of tours with minimum cardinality constrained by $f_2^R(|S_k|), f_2(|S_k|)$ and $g(|S_k|)$, respectively. Clearly, we have:

$$|\mathcal{M}^{g*}| \leqslant |\mathcal{M}^*| \leqslant |\mathcal{M}^{R*}|. \tag{16}$$

Using similar analysis in the proof of Theorem 4.2, we know the output of Algorithm 1, $\mathcal{M}$, is subject to:

$$|\mathcal{M}| \leqslant 6 \cdot \left(\left\lceil \log_2 \frac{B/\eta_T}{B/\eta_T - 2\Delta\left(\frac{\lambda \cdot (B + \eta_C \cdot \tau_{vac}^c)}{\eta_T}\right) + 2} \right\rceil + 1 \right) \cdot |\mathcal{M}^{R*}|. \tag{17}$$

Next, we show how to construct a feasible solution $\mathcal{M}'$ meeting the constraint $f_2^R(|S_k|)$ from $|\mathcal{M}^{g*}|$. In general, we use a partition method to achieve this goal. Suppose there is a tour $P_{k'} \in \mathcal{M}^{g*}$ traversing a set of nodes $|S_{k'}|$ with travel time $\tau_P^{k'}$ located in the region I, II or III, namely:

$$\tau_P^{k'} \leqslant \frac{B}{\eta_T} - \frac{B/\eta_T}{|S_k|_2^g} |S_{k'}|. \tag{18}$$

We then greedily partition $P_{k'}$ into as few paths as possible, such that each path contains at most $\left\lfloor \frac{|S_k|_2}{|S_k|_2^g} \cdot |S_{k'}| \right\rfloor$ nodes (apparently, no operation is needed when $\tau_P^{k'}$ is located in the region I). Subsequently, for each obtained path, we connect its endpoints to the BS in order to form a new tour. Note that the travel time of each newly constructed tour is definitely no more than that of $P_{k'}$, i.e., $\tau_P^{k'}$, as the weight space is metric. To summarize, for any obtained tour $P_{k_j'}$, we have $|S_{k_j'}| \leqslant \left\lfloor \frac{|S_k|_2}{|S_k|_2^g} \cdot |S_{k'}| \right\rfloor$ and $\tau_P^{k_j'} \leqslant \tau_P^{k'}$, Hence:

$$\tau_P^{k_j'} \leqslant \tau_P^{k'} \leqslant \frac{B}{\eta_T} - \frac{B/\eta_T}{|S_k|_2^g} |S_{k'}| \leqslant \frac{B}{\eta_T} - \frac{B/\eta_T}{|S_k|_2^g} \frac{|S_k|_2^g}{|S_k|_2} |S_{k_j'}|$$
$$\leqslant \frac{B}{\eta_T} - \frac{B/\eta_T}{|S_k|_2} |S_{k_j'}|. \tag{19}$$

Therefore we conclude that $\tau_P^{k_j'}$ must belong to the region I. In this way, $|\mathcal{M}^{g*}|$ tours can be finally converted into $|\mathcal{M}'|$ tours meeting the constraint $f_2^R(|S_k|)$, and is subject to:

$$|\mathcal{M}'| \leqslant \left\lceil \frac{|S_{k'}|}{\left\lceil \frac{|S_k|_2}{|S_k|_2^g} \cdot |S_{k'}| \right\rceil} \right\rceil \cdot |\mathcal{M}^{g*}| \leqslant \left(2 \cdot \frac{|S_k|_2^g}{|S_k|_2} + 1 \right) \cdot |\mathcal{M}^{g*}|$$
$$\leqslant \left(2 \cdot \frac{B + \eta_C \cdot \tau_{vac}^c}{B \cdot \frac{\eta_C}{\eta_T} + \eta_C \cdot \tau_{vac}^c} + 1 \right) \cdot |\mathcal{M}^*|. \tag{20}$$

Note the last inequality is obtained by following Eq. (16). Each tour in $|\mathcal{M}'|$ has a travel time feasible for region I. Besides, it is clear that:

$$|\mathcal{M}^{R*}| \leqslant |\mathcal{M}'| \tag{21}$$

since $\mathcal{M}^{R*}$ is optimal.

Combining Eqs. (17), (20) and (21) will give the result. $\square$

Theorem 4.4. *Given that* $\eta_C > \eta_T$, *Algorithm 1 for MinMCP-R achieves* $6 \cdot \left(2 \cdot \frac{B \cdot \frac{\eta_C}{\eta_T} + \eta_C \cdot \tau_{vac}^c}{B + \eta_C \cdot \tau_{vac}^c} + 1 \right) \left(\left\lceil \log_2 \frac{B/\eta_T}{B/\eta_T - 2\Delta\left(\frac{\lambda \cdot \left(B \cdot \frac{\eta_C}{\eta_T} + \eta_C \cdot \tau_{vac}^c\right)}{\eta_T}\right) + 2} \right\rceil + 1 \right)$- *approximation.*

Proof. For the case where $\eta_C > \eta_T$, the curve $f_2(|S_k|)$ is convex as is shown in Fig. 4. As a result, the intersection point $|S_k|_2^g$ of the line $f_2^R(|S_k|)$, which is tangent to the horizontal axis at point $|S_k| = 0$, is smaller than $|S_k|_2$. Note that $f_2^R(|S_k|)$ is one of the outputs of Algorithm 1. Moreover, the line $g(|S_k|)$ connects the two end points $|S_k| = 0$ and $|S_k| = |S_k| = 0$ of the curve $f_2(|S_k|)$. As is depicted in Fig. 4, $f_2(|S_k|), f_2^R(|S_k|)$ and $g(|S_k|)$ result in three regions, namely, I, II and III. Among there regions, I, II are feasible for $f_2(|S_k|)$ while III is not.

Denote by $\mathcal{M}^{R*}$, $\mathcal{M}^*$ and $\mathcal{M}^{g*}$ the optimal tours with minimum cardinality constrained by $f_2^R(|S_k|), f_2(|S_k|)$ and $g(|S_k|)$, respectively. We apply similar techniques used in the proof of Theorem 4.3, and therefore, transform each tour in $g(|S_k|)$ into at most $\left(2 \cdot \frac{|S_k|_2}{|S_k|_2^g} + 1 \right)$ ones, each of which is valid with respect to constraint $f_2^R(|S_k|)$. Hence,

$$|\mathcal{M}^{R*}| \leqslant \left(2 \cdot \frac{|S_k|_2}{|S_k|_2^g} + 1 \right) \cdot |\mathcal{M}^{g*}|$$
$$\leqslant \left(2 \cdot \frac{B \cdot \frac{\eta_C}{\eta_T} + \eta_C \cdot \tau_{vac}^c}{B + \eta_C \cdot \tau_{vac}^c} + 1 \right) \cdot |\mathcal{M}^*|. \tag{22}$$

Recall that $\mathcal{M}$, one of the outputs of Algorithm 1, is subject to

$$|\mathcal{M}| \leqslant 6 \cdot \left(\left\lceil \log_2 \frac{B/\eta_T}{B/\eta_T - 2\Delta\left(\frac{\lambda \cdot \left(B \cdot \frac{\eta_C}{\eta_T} + \eta_C \cdot \tau_{vac}^c\right)}{\eta_T}\right) + 2} \right\rceil + 1 \right)$$
$$\cdot |\mathcal{M}^{R*}| \tag{23}$$

Combining Eqs. (22) and (23) follows the result. $\square$

4.5. Approximation algorithm for MinMCP

The core idea of our solution is to substitute the output of Algorithm 1, $f_2^R(|S_k|)$ for the constraint $f_2(|S_k|)$. MinMCP is therefore reformulated as a minimization problem subject to two linear constraints.

Define $|S_k|_1 = \frac{\alpha - \tau_{vac}^c}{\lambda \cdot \alpha}$ ($f_1(|S_k|_1) = 0$). If $\eta_C \leqslant \eta_T$, define $|S_k|_2^R = \frac{B}{\lambda \cdot (B + \eta_C \cdot \tau_{vac}^c)}$; otherwise, define $|S_k|_2^R = \frac{B}{\lambda \cdot \left(B \cdot \frac{\eta_C}{\eta_T} + \eta_C \cdot \tau_{vac}^c \right)}$. Hence, the output of Algorithm 1 $f_2^R(|S_k|)$ can be rewritten as $f_2^R(|S_k|) = \frac{B}{\eta_T} - \frac{B}{\eta_T} \cdot \frac{1}{|S_k|_2^R} \cdot |S_k|$. Moreover, define $|S_k|^\cap = \frac{\alpha - \tau_{vac}^c - B/\eta_T}{(\alpha - \tau_{vac}^c)/|S_k|_1 - (B/\eta_T)/|S_k|_2^R}$.

The pseudo-codes of the algorithm for MinMCP can be found in Algorithm 2. Note that at Step 8 and the final step, we employ the Nearest Neighbor Algorithm for TSP to further reduce the length of each obtained tour. This improvement leads to a better performance than that of Algorithm 2 proposed in [1].

4.6. Analysis of the approximation algorithm for MinMCP

In this section, we mainly analyze the performance of the approximation algorithm for MinMCP proposed in Algorithm 2.

Generally speaking, we derive the approximation ratio for four different cases, and formally present the theoretical results in the following four theorems.

Theorem 4.5. *Given that* $\alpha - \tau_{vac}^c \leqslant \frac{B}{\eta_T}$ *and* $|S_k|_1 \leqslant |S_k|_2^R$, *Algorithm 2 for MinMCP achieves* $6 \cdot \left(\left\lceil \log_2 \frac{\alpha - \tau_{vac}^c}{\alpha - \tau_{vac}^c - 2\Delta(\lambda \cdot \alpha) + 2} \right\rceil + 1 \right)$*-approximation.*

Algorithm 2. Algorithm for MinMCP

Input: The metric space $\mathcal{W}$, the constraints $f_1(|S_k|)$ and $f_2(|S_k|)$, parameters $\eta_C, \eta_T, \lambda, \alpha, B, \tau_{vac}^c, |S_k|_1, |S_k|_2^R$ and $|S_k|^\cap$

Output The set of tours $\mathcal{M}$

1 begin

2   **if** $\alpha - \tau_{vac}^c \leqslant \frac{B}{\eta_T}$ and $|S_k|_1 \leqslant |S_k|_2^R$ **then**

3   Apply $\lambda \cdot \alpha$-Constant Transformation on $\mathcal{W}$. Run the algorithm for DVRP in the newly obtained metric space with distance bound $\alpha - \tau_{vac}^c$, and get the set of tours $\mathcal{M}$;

4

5 else if $\alpha - \tau_{vac}^c \geqslant \frac{B}{\eta_T}$ and $|S_k|_1 > |S_k|_2^R$, or $\alpha - \tau_{vac}^c > \frac{B}{\eta_T}$ and $|S_k|_1 \geqslant |S_k|_2^R$ **then**

6   Call Algorithm 1 for MinMCP-R, and obtain the set of tours $\mathcal{M}$;

7   **else if** $\alpha - \tau_{vac}^c < \frac{B}{\eta_T}$ and $|S_k|_1 > |S_k|_2^R$ **then**

8   Apply $\lambda \cdot \alpha$-Constant Transformation on $\mathcal{W}$. Run the algorithm for DVRP in the newly obtained metric space with distance bound $\alpha - \tau_{vac}^c$, and get the set of tours $\mathcal{M}'$;

9   Employ the Nearest Neighbor Algorithm for TSP on each tour in $\mathcal{M}$ to further reduce its length;

10   **for** each tour $P_k \in \mathcal{M}'$ **do**

11   **if** $|S_k| > |S_k|^\cap$ **then**

12   Greedily partition the tour P_k (in the original metric space $\mathcal{W}$) into as few paths as possible, such that the corresponding tour of each path, obtained by appending both the end points of the path with edges from the BS, complies with the constraint $f_2(|S_k|)$ **13**   **else**

14   Call Algorithm 1 for MinMCP-R, and obtain the set of tours $\mathcal{M}'$;

15   **for** each tour $P_k \in \mathcal{M}'$ **do**

16   **if** $|S_k| > |S_k|^\cap$ **then**

17   Greedily partition the tour P_k (in the original metric space $\mathcal{W}$) into as few paths as possible, such that the corresponding tour of each path, obtained by appending both the end points of the path with edges from the BS, complies with the constraint $f_1(|S_k|)$;

18   Employ the Nearest Neighbor Algorithm for TSP on each obtained tour to further reduce its length;

19 end

Proof. We illustrate the constraints $f_1(|S_k|)$ and $f_2^R(|S_k|)$ in Fig. 5. As can be seen, given that $\alpha - \tau_{vac}^c \leqslant \frac{B}{\eta_T}$ and $|S_k|_1 \leqslant |S_k|_2^R$, the feasible region for both constraints is precisely the region I formed by the constraint $f_1(|S_k|)$. In other words, the MinMCP is reduced to the problem under the single constraint $f_1(|S_k|)$ in this case. By analysis similar to that in Theorem 4.2, we claim that Algorithm 2 achieves $6 \cdot \left(\left\lceil \log_2 \frac{\alpha - \tau_{vac}^c}{\alpha - \tau_{vac}^c - 2\Delta(\lambda \cdot \alpha) + 2} \right\rceil + 1 \right)$-approximation by further reducing the MinMCP to the DVRP. This completes the proof. $\square$
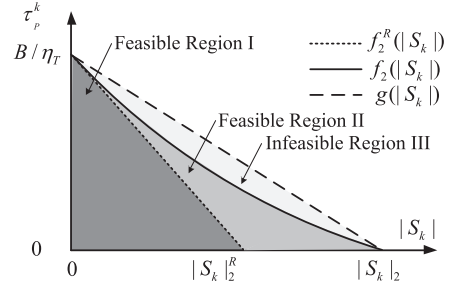

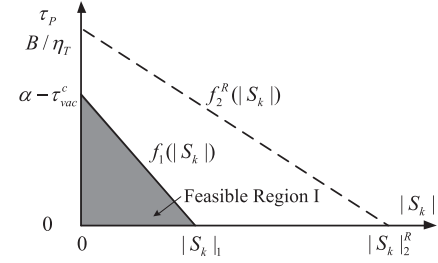**Fig. 4.** Feasible region analysis for the case where $\eta_C > \eta_T$ in MinMCP-R.

Fig. 5. Feasible region analysis for the case where $\alpha - \tau_{vac}^c \leqslant \frac{B}{\eta_T}$ and $|S_k|_1 \leqslant |S_k|_2^R$ in MinMCP.

Theorem 4.6. *Given that* $\alpha - \tau_{vac}^c \geqslant \frac{B}{\eta_T}$ *and* $|S_k|_1 > |S_k|_2^R$, *or* $\alpha - \tau_{vac}^c > \frac{B}{\eta_T}$ *and* $|S_k|_1 \geqslant |S_k|_2^R$, *Algorithm 2 for MinMCP achieves* ξ-*approximation, where* ξ *is the approximation ratio of the corresponding problem MinMCP-R.*

Proof. As the case here is similar to that of Theorem 4.5, we omit it here to save space. $\square$

Theorem 4.7. *Given that* $\alpha - \tau_{vac}^c < \frac{B}{\eta_T}$ *and* $|S_k|_1 > |S_k|_2^R$, *Algorithm 2 for MinMCP achieves* $6 \cdot \left(2 \cdot \frac{|S_k|_1}{|S_k|_2^R} + 1 \right) \left(\left\lceil \log_2 \frac{\alpha - \tau_{vac}^c}{\alpha - \tau_{vac}^c - 2\Delta(\lambda \cdot \alpha) + 2} \right\rceil + 1 \right)$-*approximation.*

Proof. Fig. 6 demonstrates the relationship between the constraints $f_2^R(|S_k|)$ and $f_1(|S_k|)$ under the given conditions. As we see, the region I is the only region feasible for both constraints $f_2^R(|S_k|)$ and $f_1(|S_k|)$. In contrast, the region II is feasible for constraint $f_1(|S_k|)$ but not for $f_2^R(|S_k|)$. Moreover, it is obvious that the obtained tours recorded by the set $\mathcal{M}$ after Step 8 in Algorithm 2 fall in the region I or II.

Let $|S_k|^\cap$ be the crossing point of the lines $f_2^R(|S_k|)$ and $f_1(|S_k|)$, namely,

$$|S_k|^\cap = \frac{\alpha - \tau_{vac}^c - B/\eta_T}{(\alpha - \tau_{vac}^c)/|S_k|^\phi - (B/\eta_T)/|S_k|_2^R}. \quad (24)$$

Apparently, we have $|S_k|^\cap < |S_k|_2^R < |S_k|_1$.

In order to make all the tours feasible for both constraints $f_2^R(|S_k|)$ and $f_1(|S_k|)$, the subsequent for loop checks each tour $P_k \in \mathcal{M}$ to see whether $|S_k|$ is greater than $|S_k|^\cap$. If the answer is no, it means that the tour P_k has already met the constraint $f_2^R(|S_k|)$, nothing needs to be done; otherwise, the tour P_k may fall into region II, thus we need to convert P_k into multiple feasible tours, as
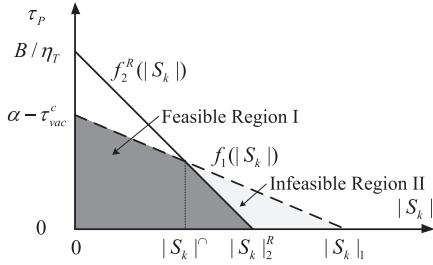
Fig. 6. Feasible region analysis for the case where $\alpha - \tau^c_{vac} < \frac{B}{\eta_T}$ and $|S_k|_1 > |S_k|_2^R$ in MinMCP.

is elaborated in Step 12. Denote by $\mathcal{M}'$ the final set of tours obtained by Algorithm 2, $\mathcal{M}^*$ the optimal set of tours for MinMCP, and $\mathcal{M}^{1*}$ the optimal set of tours under the single constraint $f_1(|S_x|)$. Following the spirit of the analysis in the proof of Theorem 4.3, we claim that the number of created tours for k is no more than $\left\lceil \frac{|S_k|}{\left\lceil \frac{|S_k|_2^R}{|S_k|_1} |S_k| \right\rceil} \right\rceil \leqslant \left(2 \cdot \frac{|S_k|_1}{|S_k|_2^R} + 1 \right)$. Therefore, we have

$$|\mathcal{M}'| \leqslant \left(2 \cdot \frac{|S_k|_1}{|S_k|_2^R} + 1 \right) \cdot |\mathcal{M}|. \tag{25}$$

Furthermore, it is easy to see

$$|\mathcal{M}| \leqslant 6 \cdot \left(\left\lceil \log_2 \frac{\alpha - \tau^c_{vac}}{\alpha - \tau^c_{vac} - 2\Delta(\lambda \cdot \alpha) + 2} \right\rceil + 1 \right) \cdot |\mathcal{M}^{1*}|. \tag{26}$$

In addition, the optimal solution for MinMCP under both constraints $f_1(|S_k|)$ and $f_2^R(|S_k|)$, $|\mathcal{M}^*|$, should by no means be greater than the optimal one for MinMCP under the single constraint $f_1(|S_k|)$, $|\mathcal{M}^{1*}|$, i.e.,

$$|\mathcal{M}^{1*}| \leqslant |\mathcal{M}^*|. \tag{27}$$

Combining Eqs. (25)(26)(27) we have

$$|\mathcal{M}'| \leqslant 6$$
$$\cdot \left(2 \cdot \frac{|S_k|_1}{|S_k|_2^R} + 1 \right) \left(\left\lceil \log_2 \frac{\alpha - \tau^c_{vac}}{\alpha - \tau^c_{vac} - 2\Delta(\lambda \cdot \alpha) + 2} \right\rceil + 1 \right)$$
$$\cdot |\mathcal{M}^*|. \tag{28}$$

This completes the proof. $\square$

Theorem 4.8. *Given that* $\alpha - \tau^c_{vac} > \frac{B}{\eta_T}$ *and* $|S_k|_1 < |S_k|_2^R$, *Algorithm 2 for MinMCP achieves* $2 \cdot \left(\frac{|S_k|_2^R}{|S_k|_1} + 1 \right) \cdot \xi$-*approximation, where* ξ *is the approximation ratio of the corresponding MinMCP-R.*

Proof. As the case concerned is similar to that of Theorem 4.7, we omit the proof here to save space. $\square$

4.7. Enhanced algorithm for MinMCP

In spite of its guaranteed approximation ratio, Algorithm 2 is still not quite efficient. Specifically, we find that the consumed energy of each MC is usually noticeably less than its battery capacity B. The root reason is that the DVRP algorithm, upon which our approximation algorithm based, is mainly designed to facilitate the derivation of approximation ratio and, therefore, sacrifices its

---

Algorithm 3. Enhanced Algorithm for MinMCP

Input: The threshold ϵ, the metric space $\mathcal{W}$, the constraints $f_1(|S_k|)$ and $f_2(|S_k|)$, parameters $\eta_C, \eta_T, \lambda, \alpha, B, \tau^c_{vac}, |S_k|_1, |S_k|_2^R$ and $|S_k|^\cap$

Output: The set of tours $\mathcal{M}$

1 begin

2 $B' = B$;

3   **while** The maximum energy consumption of the MCs does not exceed B **do**

4 $B' = 2B'$;

5   Call Algorithm 2 for MinMCP with battery capacity B' together with other related parameters, and obtain the set of tours $\mathcal{M}$;

6   Using binary search method to find the maximum battery capacity B'' that guarantees the maximum consumed energy of each MC being less than B. The initial search range is $[B'/2, B']$, and the search stops when the gap between two successive values of B'' is smaller than ϵB;

7 end

---

performance to some extent. This motivates us to further improve the approximation algorithm for MinMCP.

We present the details of the enhanced algorithm in Algorithm 3. Basically, this algorithm attempts to minimize the number of MCs by augmenting the input battery capacity as much as possible, while guaranteeing that the maximum consumed energy of each MC is less than the given battery capacity B.

It is easy to see that the output of the enhanced algorithm should be at least as good as that of the original approximation algorithm. We thus have the following theorem.

Theorem 4.9. *Algorithm 3 achieves an approximation ratio no more than that of Algorithm 2.*

5. Discussion

In this paper, we assumes that the energy consumption rate of each sensor node is constant and uniform. This assumption is, however, still somewhat strict, and not general enough. In this section, we discuss how to extend the proposed algorithms to more general cases where sensor nodes have nonuniform energy consumption rates.

Generally speaking, the nonuniformity of energy consumption rates will result in the change of constraints in MinMCP, and therefore make the problem harder to be tackled. Suppose the energy consumption rate for the sensor node v_i is p_w^i, then it can be easily derived that the two constraints in MinMCP now become

$$\tau_P^k \leqslant (\alpha - \tau^c_{vac}) - \alpha \cdot \sum_{v_i \in S_k} \frac{p_w^i}{U}$$

and

$$\tau_P^k \leqslant \frac{B - (B + \eta_C \cdot \tau^c_{vac}) \cdot \sum_{v_i \in S_k} \frac{p_w^i}{U}}{\eta_T + (\eta_C - \eta_T) \cdot \sum_{v_i \in S_k} \frac{p_w^i}{U}}$$

respectively, where $\alpha = \min_{v_i \in S_k} \frac{U \cdot (E_{max} - E_{min})}{p_w^i \cdot (U - p_w^i)}$.

For the second constraint, we can first apply techniques similar to that in the proof of Theorem 4.3 to approximate the constraint by a new one in the form of $\tau_P^k \leqslant c_1 - c_2 \cdot \sum_{v_i \in S_k} \frac{p_w^i}{U}$ (c_1 and c_2 are
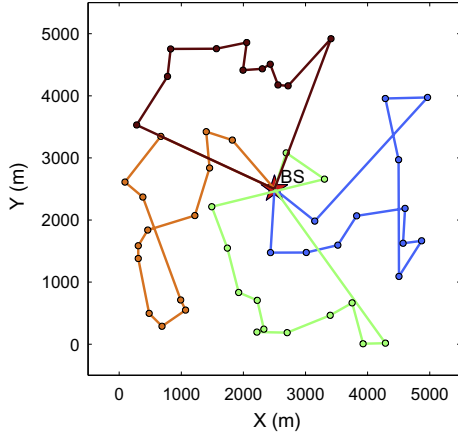
Fig. 7. An instance to the enhanced approximation algorithm for MinMCP when $B = 300$ KJ.
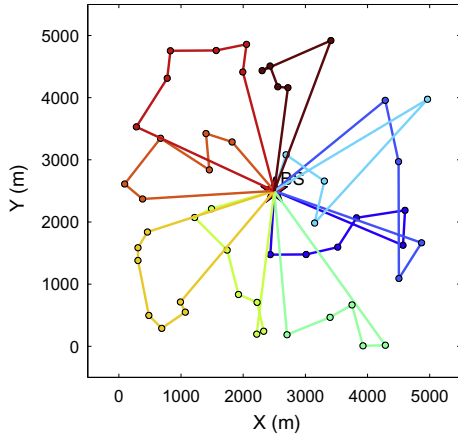

Fig. 8. An instance to the enhanced approximation algorithm for MinMCP when $B = 180$ KJ.

positive constants), then employ an extended transformation technique based on γ-Constant Transformation to further convert the constraint to the form of $\tau_P^k \leqslant c_3$, where c_3 is a constant. The original constraint is thus transformed to the traditional constraint of DVRP.

On the contrary, the first constraint is harder to be treated. This is because α is not a constant but a variable relating to the energy consumption rates of the nodes contained in the visiting set of sensor nodes S_k of the MC k. In the future work, we will devise new approximation approaches to deal with this problem, as well as the original problem when considering both of the constraints.

6. Simulation results

In this section, we present simulation results to verify our theoretical findings. We first introduce the evaluation setup, followed by the description of the baseline algorithm. Next, we illustrate an instance of the enhanced MinMCP algorithm, and then evaluate the performance of the proposed algorithms in terms of the battery capacity $B, E_{max} - E_{min}$ for sensor nodes, energy transfer rate U, charging power for MCs η_C and number of sensor nodes. For the evaluation regarding these parameters, every point on the plotted figures stands for the average value over that of 100 randomly generated topologies.
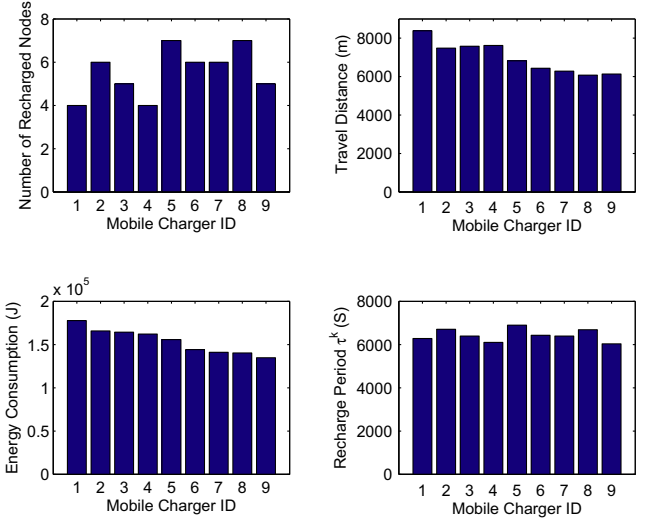

Fig. 9. Critical parameters of each MC when $B = 180$ KJ.

6.1. Evaluation Setup

We randomly distribute 50 sensor nodes in a 5 km × 5 km 2D Euclidian region throughout the simulations. Any pair of nodes can reach each other through a direct path. The base station is assumed to be located at $(2500 \text{ m}, 2500 \text{ m})$. Unless otherwise specified, we use the following parameter settings as in [14]: the traveling speed of MCs is $V = 5$ m/s, $p_w = 200$ mW, $E_{max} = 10.8$ kJ, $E_{min} = 540$ J, $U = 5$ W, $\eta_C = 110$ W, $\eta_T = 100$ W, $B = 500$ KJ and $\tau_{vac}^c = 1$ hour.

6.2. Baseline setup

Though the algorithm proposed in [22] is related to our work, it is not appropriate to use it directly for comparison. On the one hand, it is only suitable for 1D sensor networks. On the other hand, it adopts a different assumption, namely, MCs can intentionally gather at a rendezvous point to recharge others or to be recharged without energy loss. This assumption finally leads to a completely different scheme compared with ours. For this reason, we construct the following baseline algorithm by borrowing ideas of [22] for comparison. That is, all the MCs dictated by this algorithm have uniform schedule periods, which means that the MCs that finish the charging tasks earlier have to wait at BS for the returns of other MCs before starting the next trip. The chargers plan their routes in sequence. For each charger, it consistently chooses the nearest sensor node that is not chosen by the former chargers to charge after its departure from the BS. At each step, the charger checks whether its residual energy can sustain its next move to the next node and returning back to the BS. If not, the charger goes back to the BS immediately. The length of the schedule period of each charger is set to be the average length of the schedule periods determined by our algorithm for MinMCP, such that the renewable energy cycle of each sensor node can be guaranteed.

6.3. Performance evaluation

6.3.1. An Instance to the enhanced approximation algorithm for MinMCP

Fig. 7 illustrates the obtained 4 tours of MCs (marked in different colors) for a MinMCP instance given $B = 300$ KJ. However, for $B = 180$ KJ, the number of MCs needed increases to 9, as shown in Fig. 8. Note that, the Nearest Neighbor Algorithm for TSP has

been employed for each tour to further reduce its length, as shown in Algorithm 2.

For the case where $B = 180$ KJ, we show the number of charged sensor nodes, total travel distance, energy consumption and recharge period of each MC in Fig. 9. Note that we set $\tau_{vac}^k = \tau_{vac}^c$ for each MC, and sort the IDs of the MCs according to their energy consumption in a descending order. It can be seen that energy consumptions are roughly balanced among MCs, and none of them exceeds the maximum battery capacity, i.e., 180 KJ. Another important observation is that the recharge period τ^k is jointly determined by the number of recharged sensor nodes and the travel distance, rather than solely by one of them. In general, the travel distance plays a more important role than the number of recharged nodes in the total energy consumption of MCs. For example, the 5_{th} MC, which has the largest energy consumption, travels the longest distance but only recharges 3 sensor nodes. Besides, throughout the recharge period, none of the energy levels of sensor nodes drops below E_{min}, which can be confirmed by checking the conditions described in Eq. (3) and Inequality (4).

6.3.2. Impact of battery capacity (B)

In this case, we vary the maximum energy capacity B between [200 KJ, 600 KJ] to evaluate its impact on the required number of MCs $|\mathcal{M}|$. Particularly, for each value of B, we perform Algorithm 3 under 100 randomly generated topologies, and pick the average value of $|\mathcal{M}|$.

As shown in Fig. 10, not surprisingly, the number of MCs $|\mathcal{M}|$ drops with an increasing B for all three algorithms. Among these algorithms, the number of MCs needed of the enhanced MinMCP
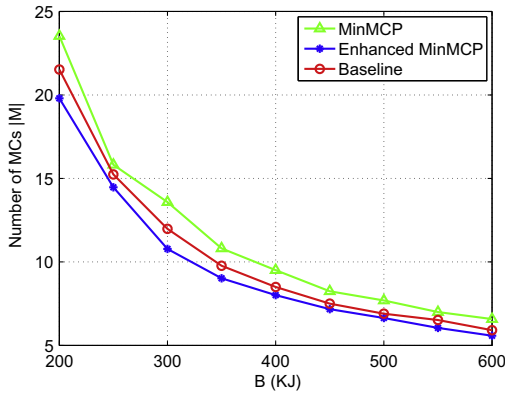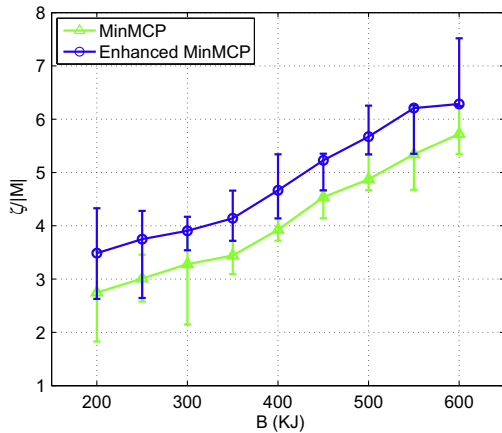

Fig. 10. Illustration of impact of B.

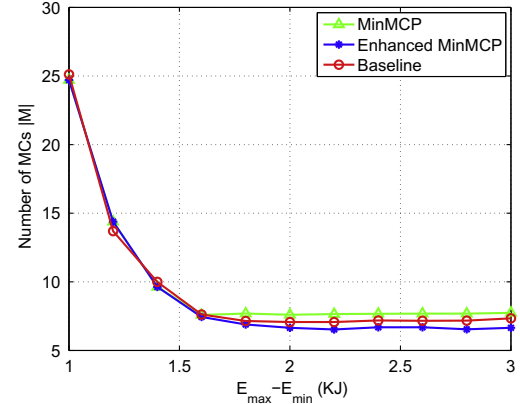**Fig. 11.** Verification of performance bound w.r.t. B.

Fig. 12. Illustration of impact of $E_{max} - E_{min}$.

algorithm is on average 6.7% and 14.8% less than that of the baseline algorithm and the MinMCP algorithm, respectively.

Let ζ be the approximation ratio given by the theoretical analysis. Though the optimal number of MCs, $|\mathcal{M}^*|$, can be hardly determined, it is certain that $|\mathcal{M}^*| \geqslant 1$. Therefore, $\zeta \geqslant |\mathcal{M}|$ or, equivalently, $\zeta/|\mathcal{M}| \geqslant 1$ can be viewed as a sufficient (but not necessary) condition to check the correctness of our theoretical analysis.

We plot the ratio of $\zeta/|\mathcal{M}|$ for the three cases in Fig. 11. Note that each point on the curves stands for the average $\zeta/|\mathcal{M}|$ over the 100 randomly generated instances, while the bars above and below the point represent the maximum and minimum values of $\zeta/|\mathcal{M}|$ among the 100 instances, respectively. It can be seen that all the values of $\zeta/|\mathcal{M}|$ for the three cases, even those minimum values, are greater than 1. This observation corroborates our theoretical findings.

6.3.3. Impact of the difference between battery capacity and minimum energy to be operational for sensor nodes ($E_{max} - E_{min}$)

We proceed to evaluate the impact of $E_{max} - E_{min}$ of sensor nodes on the minimum required number of MCs $|\mathcal{M}|$. Fig. 12 shows the trend that $|\mathcal{M}|$ drops with an increasing $E_{max} - E_{min}$ for each algorithm. Furthermore, the gaps between the three algorithms are pretty small for $E_{max} - E_{min} \leqslant 1.6$. When $E_{max} - E_{min}$ exceeds 2, the outputs of three algorithms become nearly constant. This is because in this case, the battery capacity of each sensor node is large enough to support its normal operation during a charging period
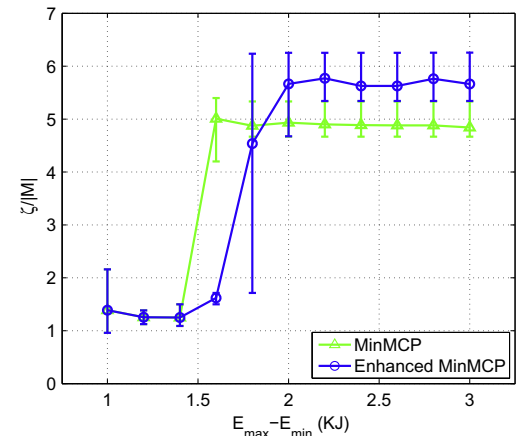

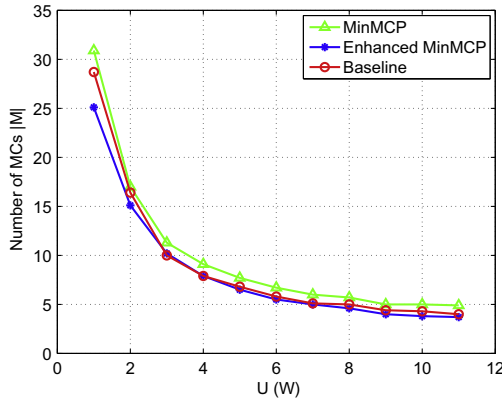**Fig. 13.** Verification of performance bound w.r.t. $E_{max} - E_{min}$.

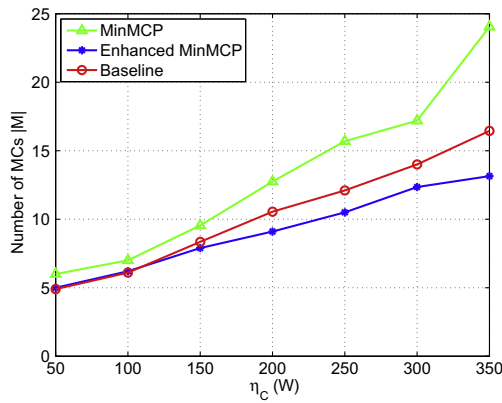**Fig. 14.** Illustration of impact of U.

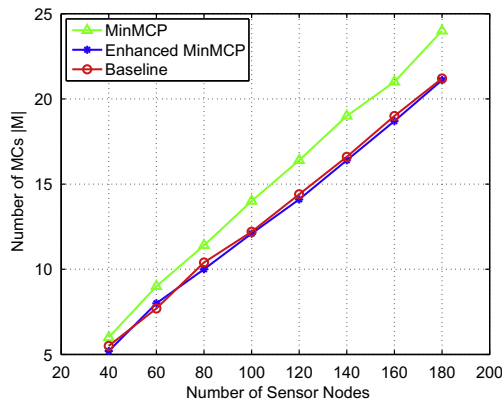**Fig. 15.** Illustration of impact of η_C.

Fig. 16. Impact of number of sensor nodes.

and, therefore, the energy capacity of the MC serves as the sole constraint.

Again, the fact that all values of $\zeta/|\mathcal{M}|$ are never less than 1, as illustrated in Fig. 13, is consistent with our theoretical results. Another important observation for this figure is that $\zeta/|\mathcal{M}|$ experiences a rapid growth when $E_{max} - E_{min}$ is 1.6 for MinMCP and 1.8 for the enhanced MinMCP algorithm. This can be ascribed to the switch from one of the four cases considered in the MinMCP algorithm to another, together with the fact that different cases have diverse approximation ratios.

6.3.4. Impact of energy transfer rate of MCs (U)

In this subsection, we study the impact of energy transfer rate U of an MC on the number of required MCs. Fig. 14 shows that when U rises from 1 W to 11 W, the number of MCs needed drops from 25.1 to 3.7 for the enhanced MinMCP algorithm, from 30.9 to 4.9 for the MinMCP algorithm and from 28.7 to 4 for the baseline algorithm. Notice that we set $E_{max} - E_{min} = 2$ KJ. The explanation of this phenomenon is straightforward. When the energy transfer rate U arises, the charging energy for each sensor node will be reduced. So does the charging time. As a result, the MCs can spare energy and time to charge more nodes, and its number is thus reduced.

6.3.5. Impact of working power of MCs for traveling (η_C)

We investigate the influence of η_C on the required number of MCs in this subsection. Intuitively, a larger η_C means an MC needs more energy to replenish the same amount of energy into the sensor node's battery, and therefore, calls for more MCs. Fig. 15 validates such intuition. Furthermore, it can be seen that the performance gaps between the three algorithms become more and more conspicuous when η_C grows. The performance gains of the enhanced MinMCP algorithm over the other two algorithms achieve 45.3% and 20.1% respectively when $\eta_C = 250$ W.

6.3.6. Impact of number of sensor nodes

We are also interested in the impact of the number of sensor nodes. As illustrated in Fig. 16, the required number of MCs for three algorithm increases steadily when the number of sensor nodes scales from 40 to 180. More precisely, the number of MCs is nearly proportional to the number of nodes, which is consistent with our intuition. Moreover, the enhanced MinMCP algorithm and the baseline algorithm need almost the same number of MCs that is roughly 14.4% less than that of the MinMCP algorithm.

7. Conclusion

In this paper, we have studied the problem of minimizing the number of energy-constrained MCs to cover a 2D WSN. We formulate the problem, and show that by applying appropriate transformations, it can be cast into the classical problem–DVRP. We not only prove the NP-hardness of the problem, but also propose approximation algorithms with proven performance bounds. The simulation results demonstrate the effectiveness of the algorithms as well as the correctness of our theoretical analysis.

In future work, we will try to improve the approximation bounds of the algorithms. Moreover, we will generalize the solution to the case in which sensor nodes have nonuniform energy consumption rates.

Appendix A. Supplementary data

Supplementary data associated with this article can be found, in the online version, at http://dx.doi.org/10.1016/j.comcom.2014.03.001.

References

[1] H. Dai, X. Wu, L. Xu, G. Chen, S. Lin, Using minimum mobile chargers to keep large-scale wireless rechargeable sensor networks running forever, in: ICCCN, 2013.

[2] V. Raghunathan, A. Kansal, J. Hsu, J. Friedman, M. Srivastava, Design considerations for solar energy harvesting wireless embedded systems, in: Proceedings of the 4th International Symposium on Information Processing in Sensor Networks, IEEE Press, 2005, p. 64.

[3] S. Meninger, J. Mur-Miranda, R. Amirtharajah, A. Chandrakasan, J. Lang, Vibration-to-electric energy conversion, IEEE Transactions on Very Large Scale Integration (VLSI) Systems 9 (1) (2001) 64–76.

[4] C. Park, P. Chou, Ambimax: autonomous energy harvesting platform for multi-supply wireless sensor nodes, in: SECON, 2006.

[5] A. Kurs, A. Karalis, M. Robert, J.D. Joannopoulos, P. Fisher, M. Soljacic, Wireless power transfer via strongly coupled magnetic resonances, Science 317 (5834) (2007) 83–86.

[6] <http://www.seattle.intel-research.net/wisp/>.

[7] H. Dai, Y. Liu, G. Chen, X. Wu, T. He, Safe charging for wireless power transfer, in: INFOCOM, 2014.

[8] <http://www.powermat.com>.

[9] <http://www.laptopmag.com/reviews/laptops/dell-latitude-3330.aspx>.

[10] <http://evworld.com/news.cfm?newsid=24420>.

[11] M. Erol-Kantarci, H. Mouftah, Suresense: sustainable wireless rechargeable sensor networks for the smart grid, Wireless Commun., IEEE 19 (3) (2012) 30–36.

[12] D. Mascareñas, E. Flynn, M. Todd, G. Park, C. Farrar, Wireless sensor technologies for monitoring civil structures, Sound Vibr. 42 (4) (2008) 16–21.

[13] B. Tong, Z. Li, G. Wang, W. Zhang, How wireless power charging technology affects sensor network deployment and routing, in: ICDCS, 2010.

[14] Y. Shi, L. Xie, Y.T. Hou, H.D. Sherali, On renewable sensor networks with wireless energy transfer, in: INFOCOM, 2011.

[15] Z. Li, Y. Peng, W. Zhang, D. Qiao, J-RoC: a joint routing and charging scheme to prolong sensor network lifetime, in: IPSN, 2011.

[16] K. Li, H. Luan, C. Shen, Qi-ferry: energy-constrained wireless charging in wireless sensor networks, in: WCNC, 2012.

[17] C. Farrar, G. Park, M. Todd, Sensing network paradigms for structural health monitoring, New Dev. Sensing Technol. Struct. Health Monitor. (2011) 137–157.

[18] H. Dai, L. Jiang, X. Wu, D.K. Yau, G. Chen, S. Tang, Near optimal charging and scheduling scheme for stochastic event capture with rechargeable sensors, in: MASS, 2013.

[19] S. He, J. Chen, F. Jiang, D.K.Y. Yau, G. Xing, Y. Sun, Energy provisioning in wireless rechargeable sensor networks, in: INFOCOM, 2011.

[20] H. Dai, X. Wu, L. Xu, G. Chen, Practical scheduling for stochastic event capture in wireless rechargeable sensor networks, in: WCNC, 2013.

[21] H. Dai, L. Xu, X. Wu, C. Dong, G. Chen, Impact of mobility on energy provisioning in wireless rechargeable sensor networks, in: WCNC, 2013.

[22] S. Zhang, J. Wu, S. Lu, Collaborative mobile charging for sensor networks, in: MASS, 2012.

[23] M. Zhao, J. Li, Y. Yang, Joint mobile energy replenishment and data gathering in wireless rechargeable sensor networks, in: ITC, 2011.

[24] S. Guo, C. Wang, Y. Yang, Mobile data gathering with wireless energy replenishment in rechargeable sensor networks, in: INFOCOM, 2013.

[25] L. Xie, Y. Shi, Y.T. Hou, W. Lou, H.D. Sherali, S.F. Midkiff, Bundling mobile base station and wireless energy transfer: Modeling and optimization, Tech. rep., 2013.

[26] L. Fu, P. Cheng, Y. Gu, J. Chen, T. He, Minimizing charging delay in wireless rechargeable sensor networks, in: INFOCOM, 2013.

[27] L. He, Y. Gu, J. Pan, T. Zhu, On-demand charging in wireless sensor networks: theories and applications, in: MASS, 2013.

[28] O. Jonah, S. Georgakopoulos, Wireless power transmission to sensors embedded in concrete via magnetic resonance, in: WAMICON, 2011.

[29] J.M. Engel, L. Zhao, Z. Fan, J. Chen, C. Liu, Smart brick-a low cost, modular wireless sensor for civil structure monitoring, in: CCCT, 2004.

[30] S.G. Taylor, K.M. Farinholt, E.B. Flynn, E. Figueiredo, D.L. Mascarenas, E.A. Moro, G. Park, M.D. Todd, C.R. Farrar, A mobile-agent-based wireless sensing network for structural monitoring applications, Measure. Sci. Technol. 20 (4) (2009) 045201.

[31] M. Buettner, R. Prasad, M. Philipose, D. Wetherall, Recognizing daily activities with rfid-based sensors, in: Ubicomp, 2009.

[32] M. Buettner, B. Greenstein, A. Sample, J. Smith, D. Wetherall, Revisiting smart dust with rfid sensor networks, in: Proceedings of the 7th ACM Workshop on Hot Topics in Networks, 2008.

[33] F. Jiang, S. He, P. Cheng, J. Chen, On optimal scheduling in wireless rechargeable sensor networks for stochastic event capture, in: MASS, 2011.

[34] V. Nagarajan, R. Ravi, Approximation algorithms for distance constrained vehicle routing problems, Networks 59 (2) (2012) 209–214.

[35] E.M. Arkin, R. Hassin, A. Levin, Approximations for minimum and min–max vehicle routing problems, J. Algorithms 59 (1) (2006) 1–18.